DiffKillR:

Killing and **R**ecreating **Diff**eomorphisms for Cell Annotation in Dense Microscopy Images

Presenter: Chen Liu

Krishnaswamy Lab, Yale University

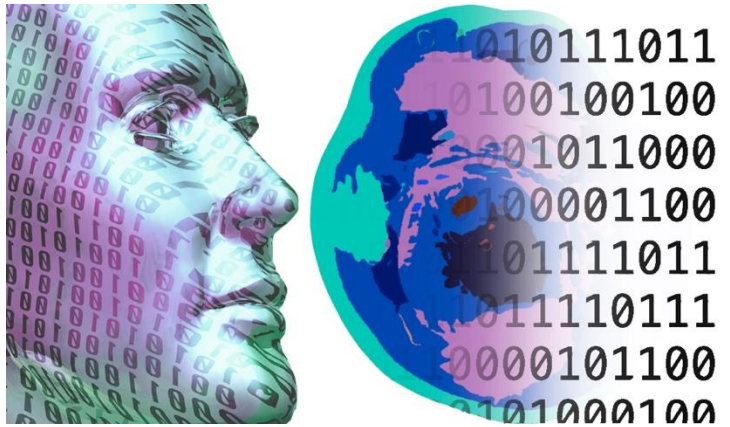

DiffKillR: Killing and Recreating Diffeomorphisms for Cell Annotation in Dense Microscopy Images

Chen Liu[1*] **Danqi Liao**[1*] **Alejandro Parada-Mayorga**[2*]
Alejandro Ribeiro[3] **Marcello DiStasio**[1] **Smita Krishnaswamy**[1]

[1]Yale University [2]University of Colorado Denver [3]University of Pennsylvania

* These authors are joint first authors.
Please direct correspondence to: smita.krishnaswamy@yale.edu.

50th IEEE International Conference on Acoustics, Speech, and Signal Processing (ICASSP 2025)

Track: Biomedical Signal and Image Processing

Motivation

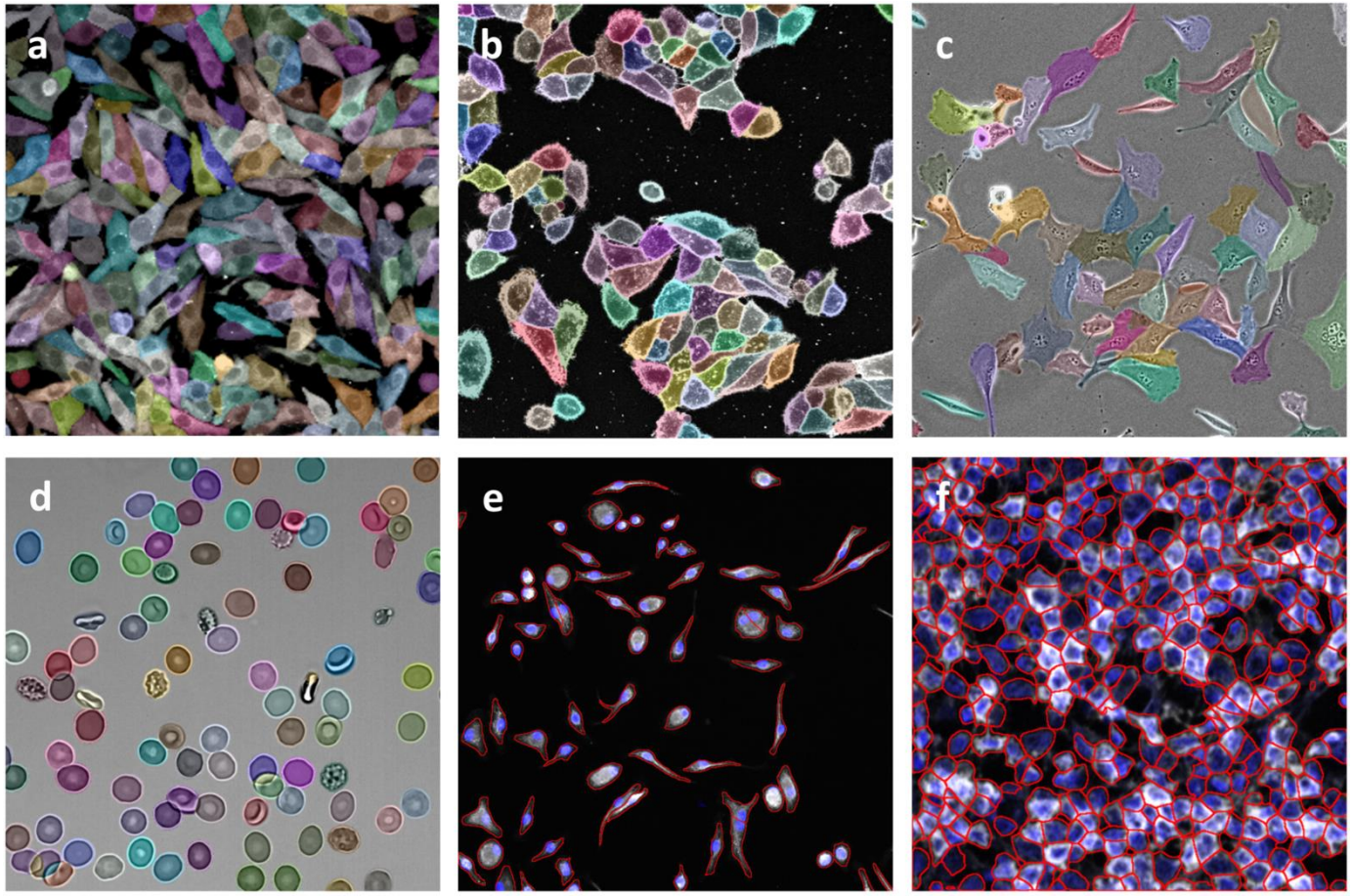

Image Credit to
Cellpose: deep learning-based, generic cell segmentation

Microscopy Image Analysis

- **Heterogeneous**
  - shape
  - appearance
  - morphology
  - modality
- **Diverse Tasks**
  - Cell Counting
  - Orientation Prediction
  - Segmentation
    - nuclei
    - cytoplasm
    - subcellular structures
  - Many others
- **Extremely Laborious**

Preliminaries

Diffeomorphisms

"A diffeomorphism is a map between manifolds which is differentiable and has a differentiable inverse."

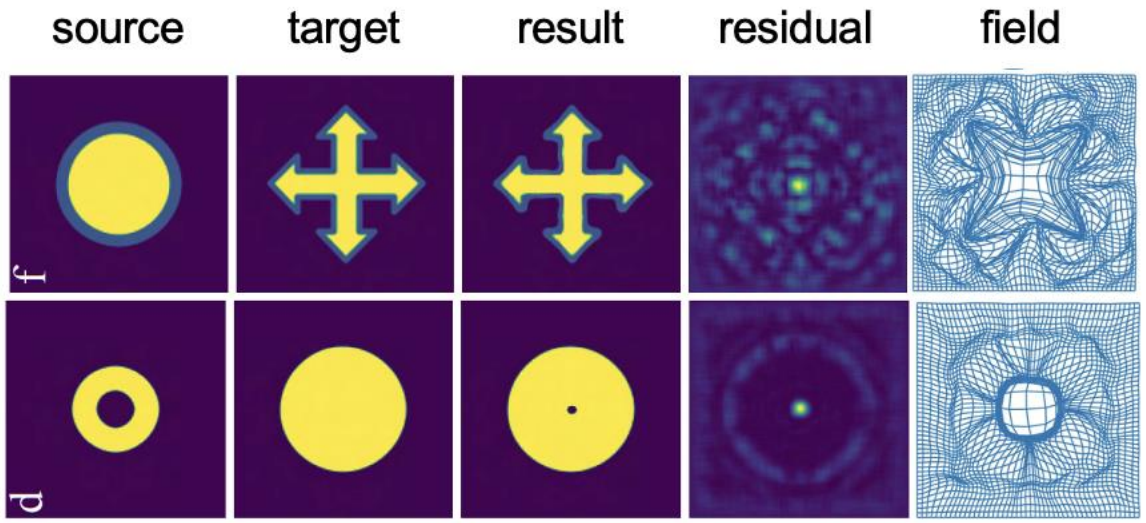

Examples of diffeomorphisms

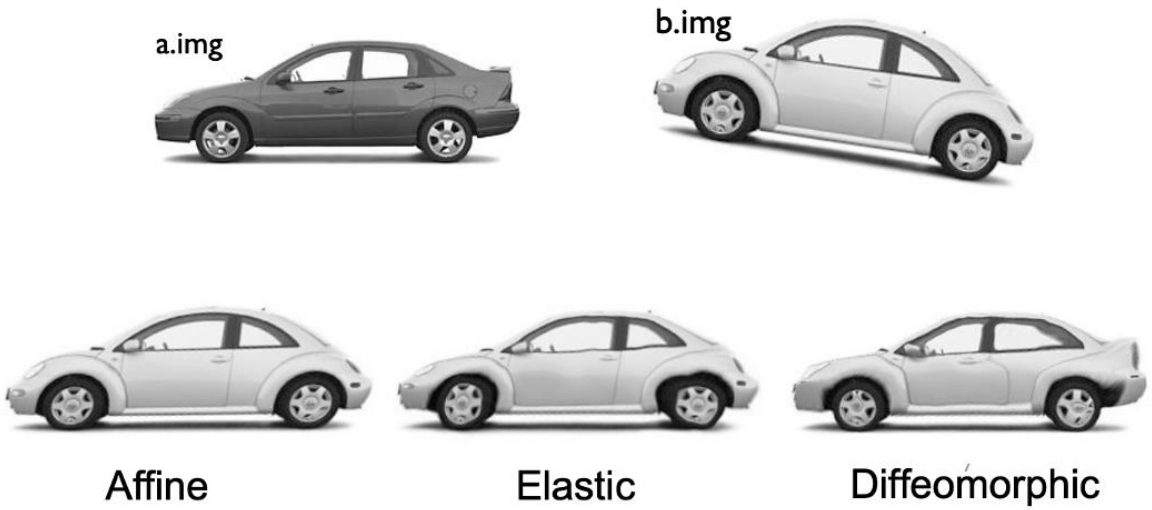

Diffeomorphisms allow local warpings

Methods (1/3)

DiffKillR: **Kill**ing and **R**ecreating **Diff**eomorphisms

Intuition: Cells exhibit diverse shapes, poses, and morphometric features, but notably, **a small set of archetypes can represent most cells**.

Remark 1: When two cells are **sufficiently similar**, differing only by a diffeomorphism, we can **compute the warping field** between them. This enables a pixel-perfect mapping of annotation from one cell to the other.

Remark 2: To achieve this, we need a way to measure such "**similarity**" that is invariant to diffeomorphisms.

Methods (2/3)

DiffKillR: **Kill**ing and **R**ecreating **Diff**eomorphisms

DiffKillR is a novel framework that reframes cell annotation as the combination of **archetype matching** and **image registration** tasks.

- Using a small set of annotated archetypes, DiffKillR efficiently propagates annotations across large microscopy images, reducing the need for extensive manual labeling.

- More importantly, it is suitable for any type of pixel-level annotation.

Methods (3/3)

DiffKillR: **Kill**ing and **R**ecreating **Diff**eomorphisms

Remark 1: When two cells are sufficiently similar, differing only by a **diffeomorphism**, we can compute the **warping field** between them. This enables a pixel-perfect mapping of annotation from one cell to the other.

→ **DiffeoMappingNet**

Sensitive to Diffeomorphisms

Remark 2: To achieve this, we need a way to measure such "**similarity**" that is invariant to diffeomorphisms.

→ **DiffeoInvariantNet**

Invariant to Diffeomorphisms

Workflow (1/3)

A small set of annotated cells forms a cell bank.
We call them “archetypal” cells, but in practice random selection would be sufficient.

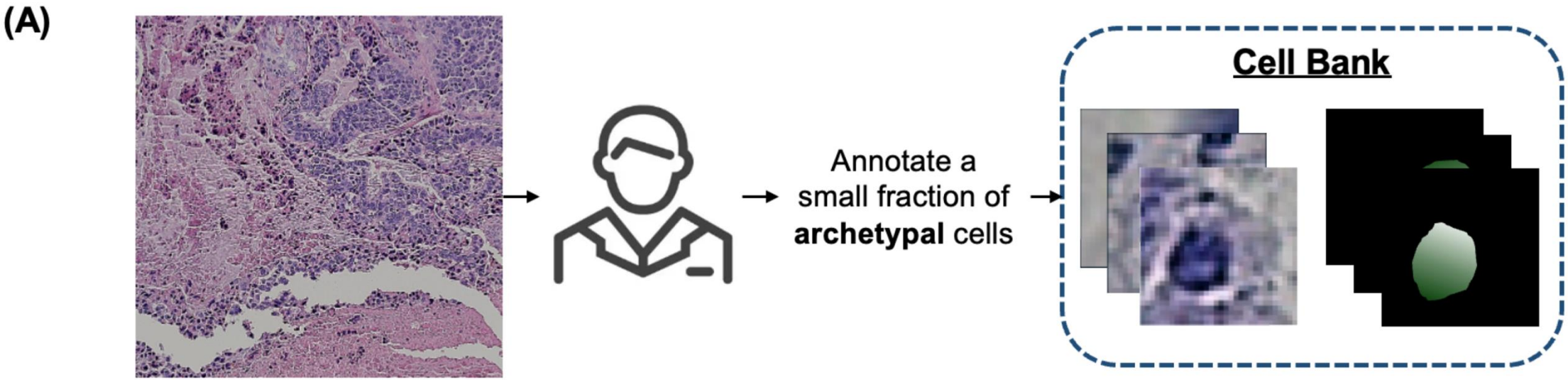

Workflow (2/3)

DiffeoInvariantNet learns a latent space that is invariant to common diffeomorphisms.
For each new cell, it finds the closest archetypal cell within the cell bank.

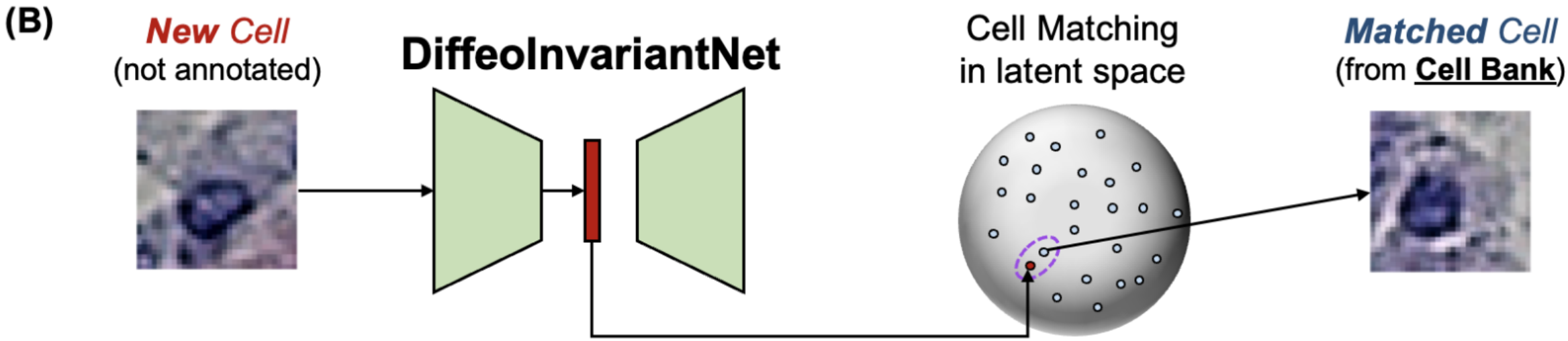

Workflow (3/3)

DiffeoMappingNet transforms the label to the new cell using the pairwise diffeomorphism computed via image registration.

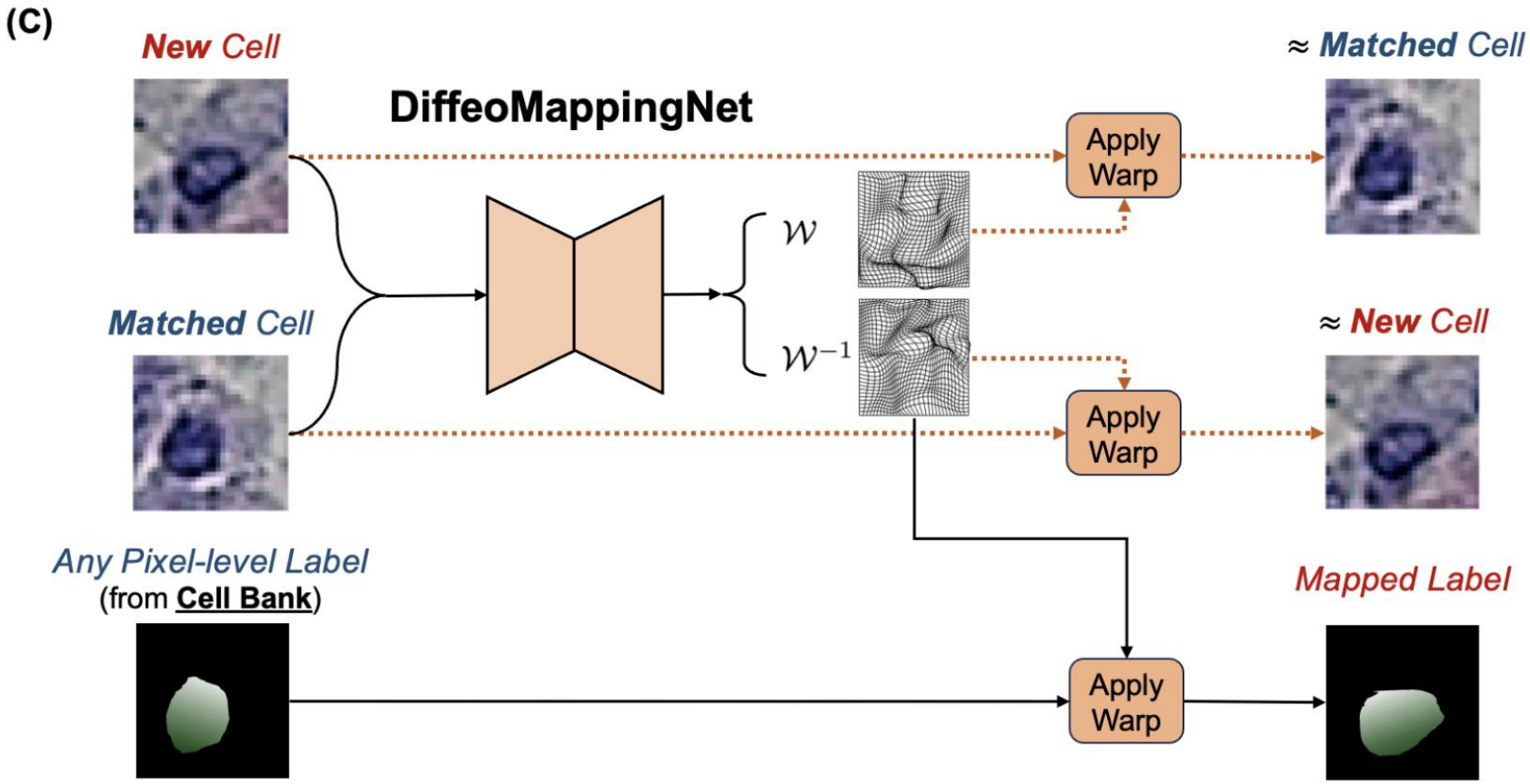

Diffeomorphisms Considered

We introduce a suite of **realistic diffeomorphisms**.

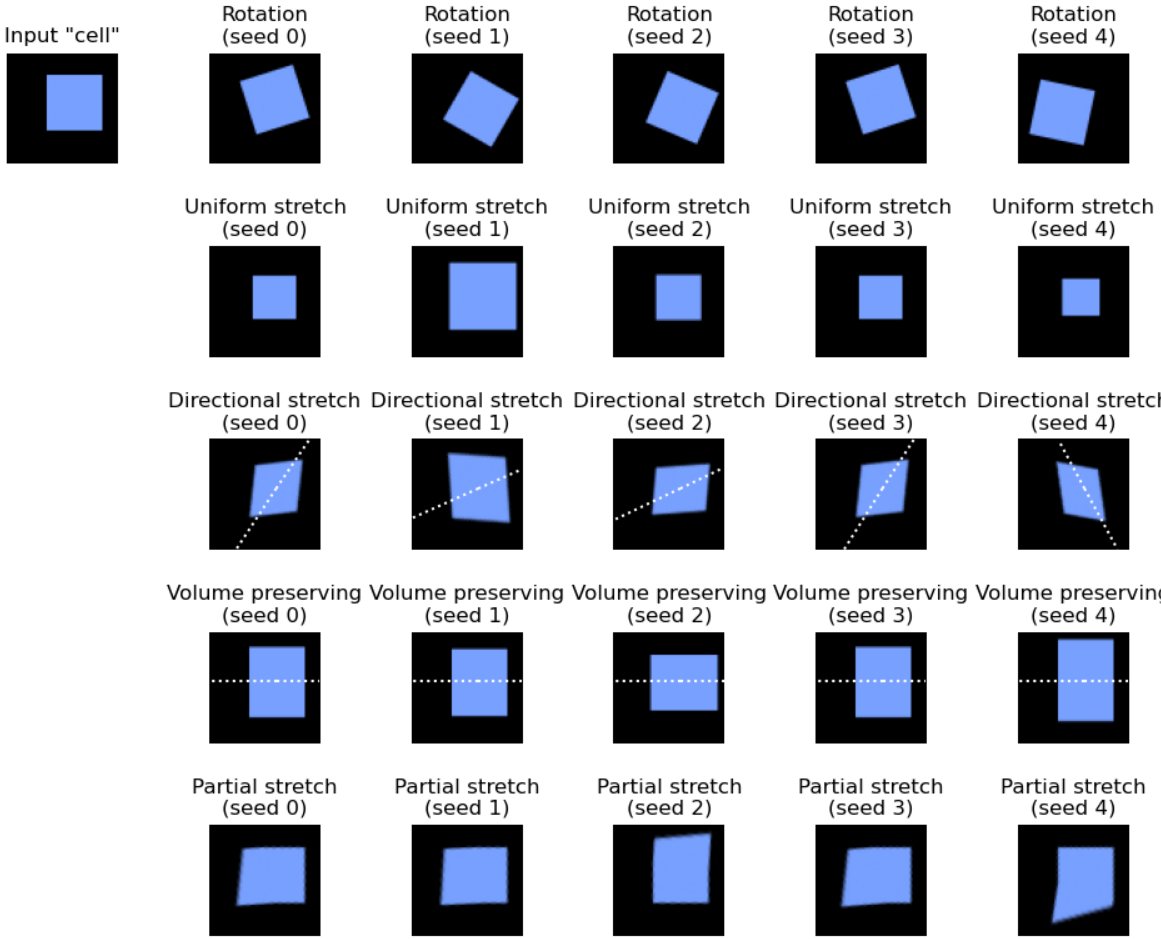

Theoretical Results (1/2)

Covers for diffeomorphism group and bandlimited deformations.

Infinite dimensional transformation can be characterized by a finite number of its realizations. Every ω-bandlimited deformation can be uniquely determined by some combinations of elements in $\hat{G}$ since there exists a constant C_0 that satisfies Equation 4.

Theorem 4.1 *[62, Adapted from Theorem 1.6] Let G be a Lie group and $\widehat{G}$ a finite subset of G. Then there exists a constant $C_0 > 0$ such that every deformation in $\mathcal{PW}_\omega(\boldsymbol{S})$ is uniquely determined by its values on $\widehat{G}$ as long as*

$$\epsilon^\star(\widehat{G}) < (C_0\omega)^{-1} \leq \epsilon_{max}(G). \tag{4}$$

$\boldsymbol{S}$: a positive definite self-adjoint operator with spectrum in [0, inf)

$\mathcal{PW}_\omega(\boldsymbol{S})$: the set of all ω-bandlimited deformations

$\epsilon_{max}(G) := \max_{g,g' \in G} d_{geo}(g, g')$ $\quad d_{geo}(\cdot,\cdot)$: geodesic distance

Theoretical Results (2/2)

Error bounds for cell matching with DiffeoInvariantNet.

For cell matching using the encoder Φ of DiffeoInvariantNet, the error between the test cell and the matched archetype cell in the latent space is bounded above by some functions of the minimal covering radius ϵ of the cell bank $\hat{G}$ and the Lipschitz constant L of the encoder.

Theorem 4.2 *Let M be the matching operator and $\mathbf{T}_{g_i}\{s_j\} = M\{\mathbf{\Phi}\{\widehat{s}\}\}$ for the test deformed cell $\widehat{s}$. If $Y_{\widehat{G}}(\epsilon) = \bigcup_{g_i \in \widehat{G}} B(g_i, \epsilon)$ is the minimum covering of G and $\mathbf{\Phi}$ is L-Lipschitz, then it follows that*

$$\|\mathbf{\Phi}\{\mathbf{T}_{g_i}\{s_j\}\} - \mathbf{\Phi}\{\widehat{s}\}\| \leq L\epsilon\|s_j\| + \mathcal{O}\left(\|\widehat{s}\|^2\right).$$

M : matching operator that matches new cell to the reference (archetypal) cell

$\mathbf{T}_{g_i}\{s_j\}$ for $i = 1, 2, \ldots, m$ and $j = 1, 2, \ldots, n$: cell bank, where m = # augmentations

$\widehat{s}$: new cell

$$M\{\mathbf{\Phi}\{\widehat{s}\}\} = \arg\min_{i,j} \|\mathbf{\Phi}\{\mathbf{T}_{g_i}\{s_j\}\} - \mathbf{\Phi}\{\widehat{s}\}\|$$

Empirical Results (1/5)

Sanity Checking the DiffeoInvariantNet

→ Reasonable cell matching results

matching cells augmented by a realistic diffeomorphism to its original version

TABLE I

CELL MATCHING ON HISTOLOGY IMAGES [30].

	MAP	1-neighbor Accuracy	3-neighbor Accuracy
Breast Cancer	0.954 ± 0.023	0.949 ± 0.009	0.912 ± 0.013
Colon Cancer	0.900 ± 0.004	0.845 ± 0.006	0.830 ± 0.007
Prostate Cancer	0.876 ± 0.012	0.799 ± 0.055	0.808 ± 0.015

Empirical Results (2/5)

Sanity Checking the DiffeoMappingNet

→ Ablating DiffeoMappingNet architecture on Synthetic Shape Registration

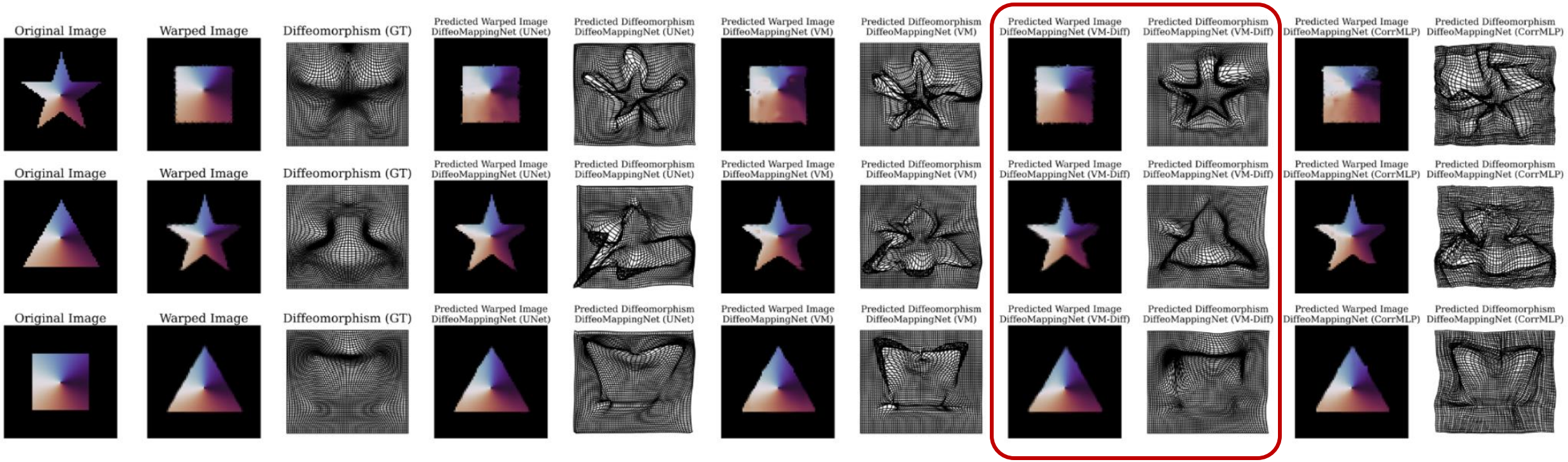

Fig. 2. Mapping diffeomorphisms of synthetic shapes with DiffeoMappingNet.

Empirical Results (2/5)

Sanity Checking the DiffeoMappingNet

→ Ablating DiffeoMappingNet architecture on Synthetic Shape Registration

TABLE II

DIFFEOMORPHISM PREDICTION ON SYNTHETIC SHAPES.

	UNet [13]	VM [25]	VM-Diff [26]	CorrMLP [27]
NCC $(\mathcal{W})$ ↑	-0.096 ± 0.961	-0.310 ± 0.899	**0.668** ± 5.397	-0.609 ± 0.527
D_{L1} $(\mathcal{W})$ ↓	1.758 ± 0.443	1.386 ± 0.232	**1.298** ± 0.258	1.356 ± 0.087
D_{L1} (image) ↓	28.367 ± 2.937	27.180 ± 5.559	**26.621** ± 3.712	26.701 ± 3.675
DSC (mask) ↑	0.964 ± 0.014	0.957 ± 0.020	0.966 ± 0.012	**0.972** ± 0.012
IoU (mask) ↑	0.931 ± 0.025	0.918 ± 0.036	0.935 ± 0.023	**0.946** ± 0.022
Runtime ↓	19.067 ± 1.424	**2.243** ± 0.130	3.220 ± 0.153	53.281 ± 1.602

Empirical Results (3/5)

Application 1: Cell Counting

TABLE III
CELL COUNTING PERFORMANCE ON HISTOLOGY IMAGES [30].

		Precision ↑	Recall ↑	F1 ↑
Breast Cancer	Blob Detection	0.488 ± 0.001	0.269 ± 0.020	0.347 ± 0.019
	DiffKillR **(ours)**, 10%	**0.500** ± 0.076	**0.719** ± 0.003	**0.585** ± 0.054
Colon Cancer	Blob Detection	0.323 ± 0.070	0.260 ± 0.044	0.288 ± 0.055
	DiffKillR **(ours)**, 10%	**0.410** ± 0.051	**0.500** ± 0.053	**0.450** ± 0.051
Prostate Cancer	Blob Detection	0.343 ± 0.038	0.264 ± 0.053	0.298 ± 0.048
	DiffKillR **(ours)**, 10%	**0.464** ± 0.077	**0.640** ± 0.046	**0.531** ± 0.034

Empirical Results (4/5)

Application 2: Cell Orientation Prediction

TABLE IV
CELL ORIENTATION PREDICTION ON EPITHELIAL CELLS.

	Hard Example Mining Ratio	D_{L1} (label) ↓	D_{θ} (label) ↓
Matching Archetype's Label	–	0.246 ± 0.036	30.29 ± 4.57
Flipping & 90-degree rotations	–	0.207 ± 0.025	19.67 ± 7.22
DiffKillR **(ours)**	0.00	$\underline{0.175} \pm 0.030$	$\underline{18.29} \pm 6.90$
	0.25	$\mathbf{0.158} \pm 0.025$	$\mathbf{17.68} \pm 6.43$
	0.50	0.189 ± 0.028	19.01 ± 7.25
	0.75	0.191 ± 0.029	19.06 ± 6.79
	1.00	0.187 ± 0.076	19.54 ± 7.21

Empirical Results (5/5)

Application 3: Few-Shot Segmentation

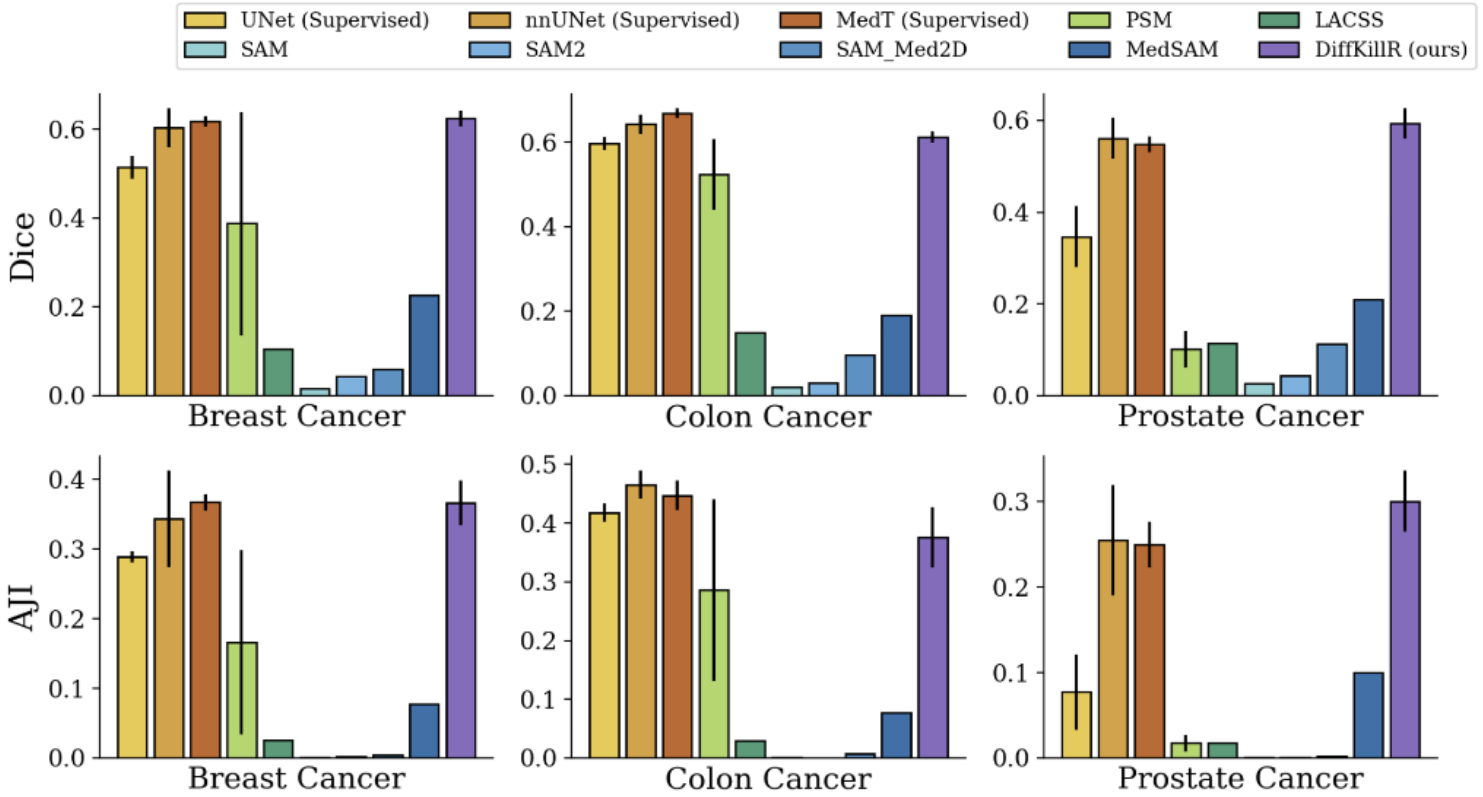

Fig. 3. Few-shot cell segmentation performance on histology images [30].

Many thanks to our team!

Chen Liu
Yale

Danqi Liao
Yale

Alejandro Parada-Mayorga
University of Colorado, Denver

Alejandro Ribeiro
University of Pennsylvania

Marcello DiStasio
Yale

Smita Krishnaswamy
Yale